Polycyclic Hydrocarbons

DOI: 10.1002/anie.201207608

Self-Assembling Decacyclene Triimides Prepared through a Regioselective Hextuple Friedel–Crafts Carbamylation**

*Toan V. Pho, Francesca M. Toma, Michael L. Chabinyc, and Fred Wudl**

Organic semiconductors have become indispensable building blocks in the quest for cost-effective production of next-generation flexible electronic devices such as organic photovoltaics and organic light-emitting diodes.[1] Despite initial concerns regarding their efficacy, the performance of p-type (hole-transporting) organic semiconductors has steadily improved to the extent of demonstrating charge carrier mobilities exceeding that of amorphous silicon.[2] Although the performance of these p-type materials has typically exceeded that of their n-type (electron-transporting) counterparts, n-type semiconductors are essential in applications, such as complementary circuits[3] and organic photovoltaics.[4] The preparation of n-type materials, however, is hampered by the intrinsic instability of organic anions in an oxidative atmosphere and the inherently low electron affinities of unsubstituted arenes/heteroarenes.[5] To produce n-type materials with increased electron affinities, the most straightforward approach involves the attachment of electron-deficient groups onto a π-conjugated core, and indeed, the diimides of rylenes such as naphthalene and perylene comprise one of the most well-studied classes of n-type organic semiconductors.[6]

Since the rylene diimides contain two electron-deficient imide groups that impart n-type character to an otherwise p-type polycyclic hydrocarbon, we focused our attention on a core structure that can support more than two imide substituents. Multiple imide substituents may increase the electron affinity of the parent material, thereby facilitating electron injection, and charge transport. However, the incorporation of multiple imide groups is a synthetic challenge, and only a few examples of tri- and tetraimides have been prepared through lengthy and/or low-yielding synthetic routes—either through oxidative Diels–Alder reactions on rylenes[7] or equatorial fusion of rylene diimides.[8] Herein, we provide a facile and efficient pathway towards novel triimides supported by the polycyclic hydrocarbon decacyclene (**1**, Scheme 1) that results in a promising class of n-type organic semiconductors.

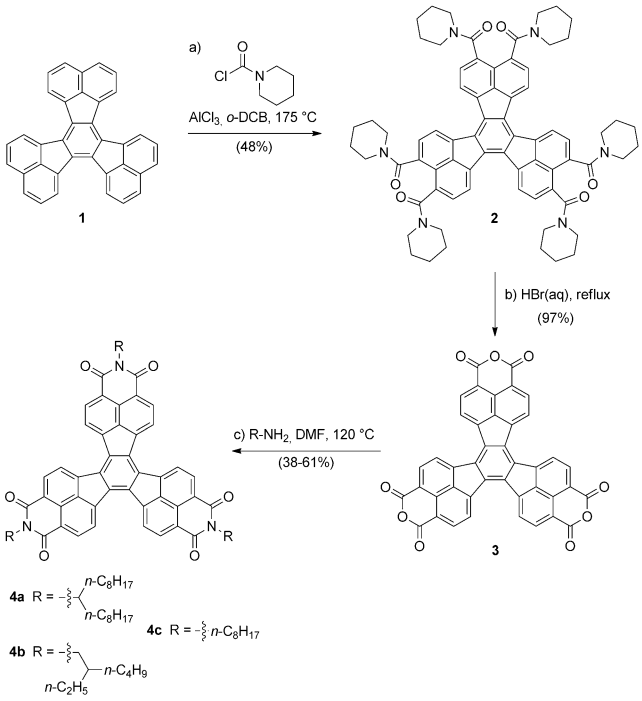

Scheme 1. Synthesis of decacyclene triimides. Reagents and conditions: a) 1-piperidinecarbonyl chloride, aluminum chloride, *o*-dichlorobenzene, 135 °C, overnight; then 175 °C, 4 days (48%); b) 48% hydrobromic acid (aq), reflux, 1 h (97%); c) primary alkylamine, *N*,*N*-dimethylformamide, 120 °C, 24 h (38–61%).

First reported at the turn of the 20th century,[9] decacyclene is a commercially available 10-ring fused polycyclic hydrocarbon with three-fold symmetry. Produced in one step from the oxidative cyclotrimerization of acenaphthene, decacyclene has been previously explored for its ability to reversibly accept up to four electrons.[10] Nevertheless, in spite of this impressive electrochemistry, the n-type properties of decacyclene derivatives have only been studied once,[11] with more attention being directed to its electron-donating character in radical cation salts.[12]

A noteworthy feature of decacyclene is its inherent potential to support multiple functional groups. For instance,

[*] T. V. Pho, F. M. Toma, Prof. M. L. Chabinyc, Prof. F. Wudl
Department of Chemistry and Biochemistry
Department of Materials, Center for Polymers and Organic Solids
University of California, Santa Barbara, CA 93106 (USA)
E-mail: wudl@chem.ucsb.edu

[**] T.V.P and F.W. thank the ConvEne IGERT Program (NSF-DGE 0801627) for financial support for DTI synthesis, and F.M.T. acknowledges financial support from the Area Science Park of Trieste and EU (TALENTS Fellowship Programme, PCOFUND-GA-2009-245574). The Center for Energy Efficient Materials, an Energy Frontier Research Center funded by the U.S. Department of Energy under award number DE-SC0001009 supported the photovoltaic research. Portions of this work were carried out using the MRL Central Facilities, which are supported by the MRSEC Program of the NSF under award number DMR 1121053; a member of the NSF-funded Materials Research Facilities Network (www.mrfn.org). Assistance from Dr. Stephan Kraemer for TEM-SAED, Dr. James Pavlovich for mass spectrometry, and Dr. Guang Wu for X-ray crystallographic analysis is also gratefully acknowledged.

Supporting information for this article is available on the WWW under http://dx.doi.org/10.1002/anie.201207608.

its hexa-*tert*-butyl derivative has been demonstrated to operate as a single molecular rotor within a supramolecular bearing at room temperature.[13] Decacyclene has also been reported to undergo a triple Friedel–Crafts acylation to afford a trialkanoyl discotic liquid-crystalline derivative.[14] Moreover, as decacyclene can be considered to be composed of three acenaphthene subunits, we surmised that the chemistry of acenaphthene could be applied directly to decacyclene, allowing for electrophilic substitution at the most reactive 3-, 4-, 9-, 10-, 15-, and 16-positions of the conjugated core. Accordingly, we devised an approach to synthesize a triimide of decacyclene by adapting the reported procedures of generating 5,6-acenaphthalimide from acenaphthene.[15]

The decacyclene triimides (DTIs) were prepared in three high-yielding steps, with the key reaction being the Friedel–Crafts carbamylation of decacyclene using 1-piperidinecarbonyl chloride to afford the hexaamide **2** (Scheme 1). The carbamylation of decacyclene was initially attempted with dimethylcarbamyl chloride using the reported conditions for the double Friedel–Crafts carbamylation of acenaphthene,[15] but an intractable mixture of materials was produced because of poor solubility. Alternatively, the use of diethylcarbamyl chloride afforded a highly soluble amide material, but de-ethylation of the ethyl groups followed by cyclization to the *N*-ethyl imide was observed under prolonged heating at high temperatures (>150 °C; see Figures S1 and S2 in the Supporting Information and additional details therein). Remarkably, switching to the cyclic piperidinecarbonyl chloride yielded a product that was significantly robust under the harsh Friedel–Crafts conditions at 175 °C and the resulting hexaamide **2** was sufficiently soluble to be purified by column chromatography.

As far as the authors know, this is the first reported instance of a *hextuple* Friedel–Crafts carbamylation of a conjugated small molecule. Furthermore, the carbamylation proceeded regioselectively with no concomitant formation of the higher amides (e.g. hepta- or octaamide). We consider this step a unique reaction, in light of the strong deactivation of the decacyclene core arising from the successive addition of each carbamyl group. Whereas multiple Friedel–Crafts alkylation reactions are known—and in many cases, uncontrollable, and hence undesirable, multiple Friedel–Crafts reactions that install carbonyl groups (carbamylation or acylation reactions) are difficult to perform because of the highly deactivating properties of the electron-deficient carbamyl/acyl groups. Indeed, while the first four carbamyl groups were readily appended onto the decacyclene core, the reactions to install the fifth and particularly the sixth carbamyl groups required several days at elevated temperatures to be completed, as indicated by thin layer chromatography.

To finish the synthesis of the DTIs, the hexaamide **2** was hydrolyzed and cyclized by hydrobromic acid to provide the trianhydride **3**. The anhydride was finally condensed with a variety of primary amines to afford the correspondingly substituted DTIs **4**. Branched amines were chosen to improve the solubility of the large π-surface DTI system, affording DTIs **4a** and **4b**. DTI **4c** with an *n*-octyl substituent was also prepared, but the exceedingly low solubility decreased the yield and hindered its chemical and physical characterization.

All of the DTIs are colored red/orange in the solid state and are yellow in dilute chloroform solutions and red/orange in concentrated solutions. UV/Vis absorption studies of DTIs **4a** and **4b** displayed strong absorption bands across the visible region from about 300–550 nm (Figure 1a). Due to its three-fold symmetry, the DTIs have doubly degenerate

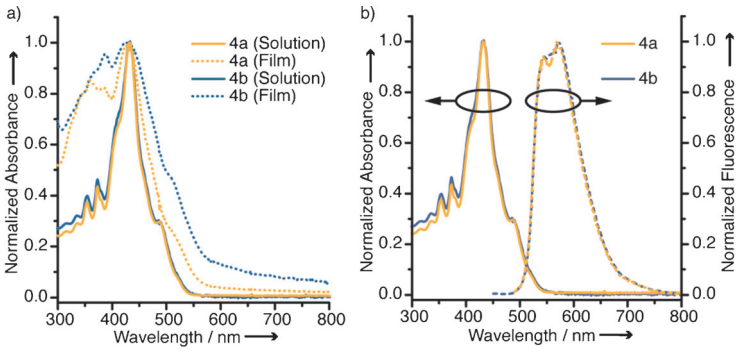

Figure 1. Optical properties of the decacyclene triimides. a) UV/Vis absorption spectra of DTIs **4a** (orange) and **4b** (blue) in chloroform solution (solid lines) and in the solid state (dotted lines); b) UV/Vis absorption (solid lines) and fluorescence (dashed lines) spectra of DTIs **4a** (orange) and **4b** (blue) in chloroform.

frontier molecular orbitals, and thus, the transition from S_0 to the lowest excited state of S_1 is symmetry forbidden.[16] Therefore, the overall absorptivity of the molecule is in principle diminished, as it is associated with transitions to higher excited states. Nevertheless, the absorption coefficient at the maximum absorption wavelength of 433 nm is considerably high ($\varepsilon = 86\,900\ \text{M}^{-1}\text{cm}^{-1}$). The absorption bands in the solid state broaden significantly compared to those in solution, suggestive of considerable aggregation in the condensed state. Furthermore, the difference between the optical band gaps of DTI **4a** (2.20 eV) and **4b** (2.16 eV) indicates that DTI **4b** may aggregate more extensively than **4a**.[17] The DTIs also exhibited a weak orange-yellow fluorescence in organic solvents (e.g. chloroform and toluene; Figure 1b). The fluorescence quantum yields of DTIs **4a** and **4b** in chloroform were 8 and 11%, respectively, relative to a standard of fluorescein in 0.1M NaOH.

Cyclic voltammetry (CV) of DTIs **4a** and **4b** showed multiple reversible reduction waves with no observable oxidation waves (Figure S3). Using a ferrocene–ferrocenium (Fc/Fc^+) redox couple as an internal standard (4.80 eV below the vacuum level), lowest unoccupied molecular orbital (LUMO) levels of −3.61 and −3.63 eV were determined for DTIs **4a** and **4b**, respectively, indicating a negligible influence of the *N*-alkyl substituent on the energy levels. Highest occupied molecular orbital (HOMO) levels of −5.81 and −5.79 eV for DTIs **4a** and **4b**, respectively, were estimated from the optical band gaps. The first and second reduction steps of the DTIs give the mono- and dianions, respectively, and the ground state of the dianion is a triplet because of the

Table 1: Optoelectronic properties of the imides.

	UV/Vis Solution		Cyclic Voltammetry			DFT Calculations[g]		
	λ_{max} [nm][b]	ε [$M^{-1}cm^{-1}$][c]	HOMO [eV][d]	LUMO [eV][e]	$E_{g,opt}$ [eV][f]	HOMO [eV]	LUMO [eV]	E_g [eV]
DTI[a]	433	86900	−5.81	−3.61	2.20	−6.33	−3.37	2.96
PDI[a]	527	104600	−5.85	−3.70	2.15	−6.00	−3.46	2.54
NDI[a]	382	25600	−6.74	−3.62	3.12	−7.04	−3.41	3.63
NMI[a]	335	14800	−6.09	−2.69	3.40	−6.48	−2.41	4.07

Energy levels are referenced to vacuum. [a] *N*-9-heptadecanyl-substituted imides. [b] Maximum absorption wavelength in $CHCl_3$ solution. [c] Molar extinction coefficient at λ_{max}. [d] HOMO level calculated by subtracting the optical band gap from the electrochemical LUMO level. [e] LUMO level calculated from the onset of the reduction wave and the half-wave potential of the ferrocene internal standard. [f] Optical band gap calculated from the absorption onset in the solid state. [g] DFT calculations of the *N*-methyl substituted imides.

doubly degenerate LUMO level.[16a] Because of the low-lying LUMO, the triplet dianions of the DTIs are easily accessible through electrochemical reduction, making these materials potentially interesting for applications such as organic ferromagnets.

Despite the presence of three electron-withdrawing imide groups, the LUMO levels of the DTIs were approximately equal to (or slightly higher than) the measured LUMOs of the most well-known diimides: naphthalene diimide (NDI) and perylene diimide (PDI, Table 1). According to valence bond theory, the π electrons of decacyclene cannot be delocalized over the entire core, implying that the three acenaphthalimide units are partially independent moieties. Complete overlap of the molecular orbitals in the DTI is thus inhibited, contributing to a LUMO level that is approximately equal to those of the fully delocalized diimides. However, there is indeed some communication between the three imide groups, as evidenced by the lower LUMO level of DTI compared to that of naphthalene monoimide (NMI).

The energy levels of decacyclene and the various imide materials were further probed by density functional theory (DFT) calculations at the B3LYP/6-31G* level of theory (Figure S4). The calculations confirmed the doubly degenerate molecular orbitals of DTI and decacyclene, which is in contrast to the orbitals of PDI, NDI, and NMI. Moreover, the incompletely delocalized HOMO of decacyclene likely contributes to the success of the hextuple Friedel–Crafts carbamylation, as the addition of each carbamyl group only partially deactivates the remaining reactive positions on the ring. Indeed, DFT calculations revealed that significant electron density was still located on the reactive sites of the amide intermediates (see Figure S5). The HOMO of DTI is dominated by the HOMO of the decacyclene core, whereas the LUMO of DTI conveys elements of the LUMOs of decacyclene and NMI. Finally, the LUMOs of NDI and PDI are extensively delocalized over the entire molecule, and in contrast, the LUMO of DTI is only partially delocalized over two of the acenaphthalimide subunits, with minimal delocalization over the third acenaphthalimide unit.

Because polycyclic hydrocarbons such as decacyclene and perylene diimides are known to self-assemble into well-defined nanostructures due to strong intermolecular π–π stacking,[18] we investigated the potential self-assembly of the DTIs. As revealed by scanning electron microscopy (SEM), DTI **4a** formed hexagonal pillars approximately 1 μm wide and up to 3 μm long (Figure 2a) when drop-cast from tetrahydrofuran (THF) solution. These structures were also analyzed by high-resolution transmission electron microscopy (HRTEM, Figure 2c), which disclosed the presence of lattice fringes that supported the inherent crystallinity of the hexagonal pillars. Even though TEM-selected area electron diffraction (TEM-SAED) of a single nanostructure revealed a relatively weak scattering, the Fourier transform of the

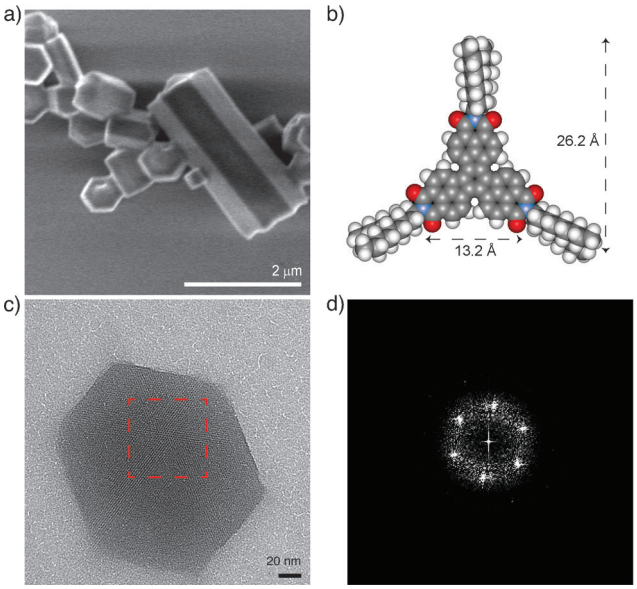

Figure 2. Self-assembly of DTI **4a**. a) SEM image of hexagonal pillars formed by DTI **4a** when drop-cast onto a silicon substrate from THF solution. The hexagonal nanostructures were preferentially oriented perpendicular to the surface. The pillars measured up to 1 μm wide and up to 3 μm long (scale bar 2 μm); b) Space-filling model of the PM3-optimized geometry of **4a** bearing *N*-9-heptadecanyl substituents. The decacyclene core measured 13.2 Å, and the entire size of the molecule (26.2 Å) was calculated by $\ell(\sqrt{3}/2)$ where ℓ is the length (30.3 Å) between two terminal methyl groups on adjacent imides; c) TEM image showing lattice fringes of a single hexagonal pillar base (scale bar 20 nm). The red square indicates the area of the image where the Fourier transform was extracted; d) Fourier transform obtained by analyzing the red square in Figure 3c. The Fourier transform showed the presence of a hexagonal pattern with a *d*-spacing of 18.5 ± 1.4 Å that supported the inherent crystallinity of the hexagonal pillars. The experimental error was calculated as the full width half maximum (FWHM) value of the intensity of the Fourier transform peaks.

highlighted area in Figure 2c showed a hexagonal pattern (Figure 2d) that is compatible with the hexagonal packing of the molecules. The *d*-spacing extracted from the Fourier transform is (18.5 ± 1.4) Å, while the calculated lengths of the DTI core and the entire DTI **4a** are 13.2 and 26.2 Å, respectively (Figure 2b). These data suggest that DTI **4a** organizes into circular stacks with a calculated radius of 17.5 Å, which correlates well with the observed *d*-spacing (see Figure S6). Because the DTI **4a** pillars tended to self-assemble perpendicular to the substrate, it was not possible to image along the longitudinal axis of the pillars by TEM-SAED. Nonetheless, DTI **4a** is expected to form π-stacks along this direction, as supported by the propensity of decacyclene to self-assemble via π–π stacking[18a] as well as our experimental observations of DTI **4b**. Interestingly, the ability of DTI **4a** to self-assemble into ordered 3D nanostructures is markedly different from similarly substituted PDIs, where the steric hindrance of the swallow-tail substituents has been known to inhibit self-assembly.[18b]

In contrast, DTI **4b** notably formed ultralong fibers with high aspect ratio when drop-cast from *o*-DCB solution. As reported in Figure 3a, these fibers were about half a micron wide (Figure 3c and Figure S7) and up to a millimeter long

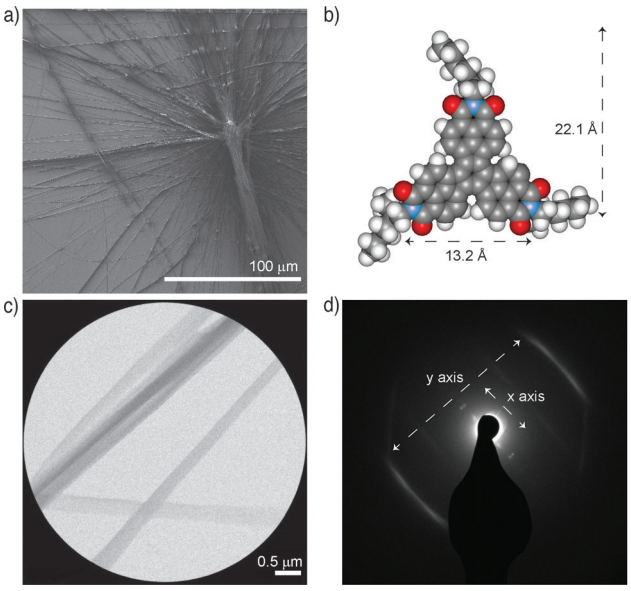

Figure 3. Self-assembly of DTI **4b**. a) SEM image of ultralong fibers formed by DTI **4b** when drop-cast onto a silicon substrate from *o*-DCB solution. The fibers were half a micron wide and up to a millimeter long and preferentially assembled into thicker bundles (scale bar 100 μm). b) Space-filling model of the PM3-optimized geometry of **4b** bearing 2-ethylhexyl substituents. The decacyclene core measured 13.2 Å, and the entire size of the molecule (22.1 Å) was calculated by $\ell(\sqrt{3}/2)$, where ℓ is the length (25.5 Å) between two terminal methyl groups of the hexyl chains on adjacent imides. c) Selected area TEM image of ultra-long fibers deposited onto a TEM carbon grid from *o*-DCB solution (scale bar 0.5 μm). d) Diffraction pattern of Figure 1c. Two *d*-spacings were observed, one (3.69 ± 0.05 Å) along the longitudinal direction (*y* axis) and another (20.8 ± 1.8 Å) along the transverse direction (*x* axis) of the fibers. The *d*-spacings were calculated with respect to a Au (111) standard, and the experimental error was calculated as the FWHM value of the intensity of the diffraction peaks.

(see Figure S8 in the Supporting Information). HRTEM displayed the presence of lattice fringes that confirmed the crystallinity of the fibers (see Figure S9), and two *d*-spacing values, one along the longitudinal fiber axis (3.69 ± 0.05 Å) and another in the transverse direction (20.8 ± 1.8 Å), were derived from TEM-SAED (Figure 3d). The calculated length of DTI **4b** is 22.1 Å (Figure 3b), indicating that the molecules are oriented with their planes along the transverse direction of the fibers, while assembling by π–π stacking along the longitudinal fiber axis (see Figure S9). When deposited from THF solution, DTI **4b** produced thicker and shorter fibers compared to those obtained from *o*-DCB solution (see Figure S10).

Self-assembly is a desirable tool in the field of organic electronics because of the possibility to pattern multidimensional platforms using a bottom-up approach. Indeed, spatial control of material building blocks is instrumental in the fabrication of structures on a multiple length scale, and this concept has been demonstrated with the DTIs. The self-assembly of the DTIs into either discrete columnar or fiberlike structures is an attractive feature for their potential use in organic semiconducting devices, where continuous crystalline domains that are characterized by π–π stacking can provide efficient pathways for charge transport. Furthermore, the DTIs with appropriately branched substituents (**4a** and **4b**) display excellent solubility ($>20\ mg\,mL^{-1}$) in organic solvents (e.g. chloroform, *o*-DCB), affirming them as promising components in solution-processable devices. The large π-surface of these materials coupled with the three electron-deficient imide groups augurs well for their electron-transporting capability.

The DTIs studied here have similar electronic levels to PCBM (LUMO = −3.7 eV and HOMO = −6.1 eV), the most commonly used acceptor in bulk heterojunction organic solar cells, suggesting that they may form type II heterojunctions with many semiconducting polymers. Indeed, preliminary photovoltaic devices fabricated using a poly(3-hexylthiophene) (P3HT):DTI **4a** blend have power conversion efficiencies (PCEs) of 1.60% (Figure 4), which greatly surpass the efficiencies (< 0.5%) of analogous P3HT cells using PDIs.[19] In detail, a short circuit current density (J_{sc}) of 4.87 mA cm^{-2}, an open circuit voltage (V_{oc}) of 0.58 V, and a fill factor (FF) of 0.57 were observed for these devices, which employed a conventional architecture of indium tin oxide (ITO)/poly(3,4-ethylenedioxythiophene):poly(styrenesulfonate) (PEDOT:PSS)/active layer/LiF/Al (see the Supporting Information). Notably, the use of PDIs as the acceptor component typically achieves FFs of at most 0.38,[19] which restricts the overall PCEs of these systems. In contrast, the high FF of the DTI **4a** devices is indicative of efficient charge extraction because of its molecular ordering.[20] Photovoltaic devices using a P3HT:DTI **4b** blend showed a PCE of 0.03%, and they exhibited significant leakage current, as demonstrated by the dark and light *J*–*V* curves at reverse biases (see Figure S11). DTI **4b** has been observed to more readily crystallize with respect to DTI **4a**, and this effect can explain the difference in performance between the two materials. Further experiments to investigate the structural and morphological properties of the solar cells as well as to optimize

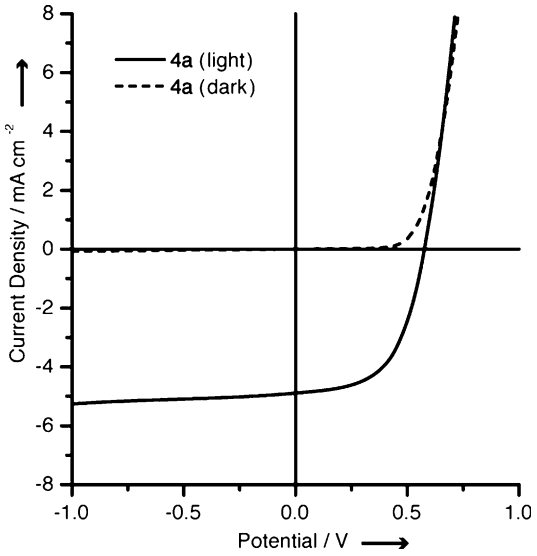

Figure 4. Current density–voltage (*J-V*) curves of P3HT:DTI photovoltaic devices utilizing DTI **4a** (light: black solid line; dark: black dashed line).

the overall efficiencies of the DTI-based devices are currently in progress.

Moreover, the precursor to the triimides, the decacyclene trianhydride **3**, is an appealing building block for multifunctional oligomeric and polymeric materials. The trianhydride is also a potentially important monomer for dendritic Kapton®-type oligomers and as a crosslinker for the high-performance polymer Kapton®, possibly making it an even stronger engineering plastic.[21]

In summary, we have developed a unique regioselective hextuple Friedel–Crafts carbamylation that allowed the facile synthesis of a new class of n-type organic semiconductors—decacyclene triimides. The success of the Friedel–Crafts reaction hinged on the crucial choice of a cyclic carbamyl group, thereby striking a fine balance between stability and solubility. Whereas branched alkyl-substituted perylene diimides are known to aggregate into bulky amorphous structures, the self-assembly of branched alkyl-substituted decacyclene triimides into ordered crystalline architectures has been shown. The large π-surface of these triimides is critical for their self-assembling properties that can be tuned to give crystalline columns or fibers by modifying the alkyl substituents. In addition, the self-assembly and the strong electron-accepting capability of the DTIs make them attractive for use in organic semiconducting devices such as field-effect transistors and photovoltaic cells. Preliminary bulk heterojunction solar cells fabricated using a P3HT:DTI **4a** blend have exhibited power conversion efficiencies of 1.6% and fill factors of 0.57, which demonstrate the promising application of these non-fullerene acceptors in organic electronics.

Experimental Section

Materials, methods, synthetic details for compounds **2** to **4**, X-ray diffraction studies on DTI **4a**, cyclic voltammograms, molecular orbital diagrams, thermal properties of the DTIs, additional SEM and TEM images, and details concerning the fabrication and characterization of the photovoltaic devices are described in the Supporting Information.

Received: September 19, 2012
Published online: December 18, 2012

Keywords: aromatic substitution · fused-ring systems · imides · polycycles · self-assembly

[1] a) A. C. Arias, J. D. MacKenzie, I. McCulloch, J. Rivnay, A. Salleo, *Chem. Rev.* **2010**, *110*, 3–24; b) F. G. Brunetti, R. Kumar, F. Wudl, *J. Mater. Chem.* **2010**, *20*, 2934–2948; c) G. Horowitz, *Adv. Mater.* **1998**, *10*, 365–377; d) C. D. Dimitrakopoulos, P. R. L. Malenfant, *Adv. Mater.* **2002**, *14*, 99–117; e) H. E. Katz, *J. Mater. Chem.* **1997**, *7*, 369–376; f) C. J. Brabec, N. S. Sariciftci, J. C. Hummelen, *Adv. Funct. Mater.* **2001**, *11*, 15–26; g) K. M. Coakley, M. D. McGehee, *Chem. Mater.* **2004**, *16*, 4533–4542; h) S. Günes, H. Neugebauer, N. S. Sariciftci, *Chem. Rev.* **2007**, *107*, 1324–1338; i) P. K. H. Ho, J.-S. Kim, J. H. Burroughes, H. Becker, S. F. Y. Li, T. M. Brown, F. Cacialli, R. H. Friend, *Nature* **2000**, *404*, 481–484.

[2] a) S. Allard, M. Forster, B. Souharce, H. Thiem, U. Scherf, *Angew. Chem.* **2008**, *120*, 4138–4167; *Angew. Chem. Int. Ed.* **2008**, *47*, 4070–4098; b) C. Wang, H. Dong, W. Hu, Y. Liu, D. Zhu, *Chem. Rev.* **2012**, *112*, 2208–2267.

[3] a) B. Crone, A. Dodabalapur, Y. Y. Lin, R. W. Filas, Z. Bao, A. LaDuca, R. Sarpeshkar, H. E. Katz, W. Li, *Nature* **2000**, *403*, 521–523; b) H. Klauk, U. Zschieschang, J. Pflaum, M. Halik, *Nature* **2007**, *445*, 745–748.

[4] a) C. J. Brabec, S. Gowrisanker, J. J. M. Halls, D. Laird, S. Jia, S. P. Williams, *Adv. Mater.* **2010**, *22*, 3839–3856; b) B. C. Thompson, J. M. J. Fréchet, *Angew. Chem.* **2008**, *120*, 62–82; *Angew. Chem. Int. Ed.* **2008**, *47*, 58–77; c) J. E. Anthony, *Chem. Mater.* **2011**, *23*, 583–590.

[5] a) C. R. Newman, C. D. Frisbie, D. A. da Silva Filho, J.-L. Brédas, P. C. Ewbank, K. R. Mann, *Chem. Mater.* **2004**, *16*, 4436–4451; b) A. R. Murphy, J. M. J. Fréchet, *Chem. Rev.* **2007**, *107*, 1066–1096.

[6] a) H. E. Katz, A. J. Lovinger, J. Johnson, C. Kloc, T. Siegrist, W. Li, Y. Y. Lin, A. Dodabalapur, *Nature* **2000**, *404*, 478–481; b) X. Zhan, A. Facchetti, S. Barlow, T. J. Marks, M. A. Ratner, M. R. Wasielewski, S. R. Marder, *Adv. Mater.* **2011**, *23*, 268–284; c) H. Yan, Z. Chen, Y. Zheng, C. Newman, J. R. Quinn, F. Dotz, M. Kastler, A. Facchetti, *Nature* **2009**, *457*, 679–686; d) J. E. Anthony, A. Facchetti, M. Heeney, S. R. Marder, X. Zhan, *Adv. Mater.* **2010**, *22*, 3876–3892; e) F. Würthner, M. Stolte, *Chem. Commun.* **2011**, *47*, 5109–5115.

[7] a) H. Langhals, S. Kirner, *Eur. J. Org. Chem.* **2000**, 365–380; b) S. Alibert-Fouet, I. Seguy, J.-F. Bobo, P. Destruel, H. Bock, *Chem. Eur. J.* **2007**, *13*, 1746–1753.

[8] a) H. Qian, Z. Wang, W. Yue, D. Zhu, *J. Am. Chem. Soc.* **2007**, *129*, 10664–10665; b) H. Qian, F. Negri, C. Wang, Z. Wang, *J. Am. Chem. Soc.* **2008**, *130*, 17970–17976; c) W. Yue, A. Lv, J. Gao, W. Jiang, L. Hao, C. Li, Y. Li, L. E. Polander, S. Barlow, W. Hu, S. Di Motta, F. Negri, S. R. Marder, Z. Wang, *J. Am. Chem. Soc.* **2012**, *134*, 5770–5773.

[9] K. Dziewoński, *Ber. Dtsch. Chem. Ges.* **1903**, *36*, 962–971.

[10] T. Saji, S. Aoyagui, *J. Electroanal. Chem.* **1979**, *102*, 139–141.

[11] K. Hirota, K. Tajima, K. Hashimoto, *Synth. Met.* **2007**, *157*, 290–296.

[12] a) J. B. Torrance, P. S. Bagus, I. Johannsen, A. I. Nazzal, S. S. P. Parkin, P. Batail, *J. Appl. Phys.* **1988**, *63*, 2962–2965; b) T. Sugano, M. Kinoshita, *Bull. Chem. Soc. Jpn.* **1989**, *62*, 2273–2278.

[13] J. K. Gimzewski, C. Joachim, R. R. Schlittler, V. Langlais, H. Tang, I. Johannsen, *Science* **1998**, *281*, 531 – 533.
[14] E. Keinan, S. Kumar, R. Moshenberg, R. Ghirlando, E. J. Wachtel, *Adv. Mater.* **1991**, *3*, 251 – 254.
[15] a) L. A. Carpino, S. Göwecke, *J. Org. Chem.* **1964**, *29*, 2824 – 2830; b) B. M. Trost, G. M. Bright, C. Frihart, D. Brittelli, *J. Am. Chem. Soc.* **1971**, *93*, 737 – 745.
[16] a) R. E. Jesse, P. Biloen, R. Prins, J. D. W. van Voorst, G. J. Hoijtink, *Mol. Phys.* **1963**, *6*, 633 – 635; b) C. J. M. Brugman, P. J. van Scherpenzeel, R. P. H. Rettschnick, G. J. Hoijtink, *J. Chem. Phys.* **1973**, *58*, 3468 – 3471.
[17] Z. Chen, B. Fimmel, F. Würthner, *Org. Biomol. Chem.* **2012**, *10*, 5845 – 5855.
[18] a) H. Wang, X. Xu, L. Li, C. Yang, H.-F. Ji, *Micro Nano Lett.* **2011**, *6*, 763 – 766; b) K. Balakrishnan, A. Datar, T. Naddo, J. Huang, R. Oitker, M. Yen, J. Zhao, L. Zang, *J. Am. Chem. Soc.* **2006**, *128*, 7390 – 7398; c) L. Zang, Y. Che, J. S. Moore, *Acc. Chem. Res.* **2008**, *41*, 1596 – 1608; d) Z. Chen, A. Lohr, C. R. Saha-Möller, F. Würthner, *Chem. Soc. Rev.* **2009**, *38*, 564 – 584.
[19] a) V. Kamm, G. Battagliarin, I. A. Howard, W. Pisula, A. Mavrinskiy, C. Li, K. Müllen, F. Laquai, *Adv. Energy Mater.* **2011**, *1*, 297 – 302; b) W. S. Shin, H.-H. Jeong, M.-K. Kim, S.-H. Jin, M.-R. Kim, J.-K. Lee, J. W. Lee, Y.-S. Gal, *J. Mater. Chem.* **2006**, *16*, 384 – 390; c) X. Guo, L. Bu, Y. Zhao, Z. Xie, Y. Geng, L. Wang, *Thin Solid Films* **2009**, *517*, 4654 – 4657.
[20] M. A. Brady, G. M. Su, M. L. Chabinyc, *Soft Matter* **2011**, *7*, 11065 – 11077.
[21] E. H. Lee in *Polyimides: Fundamentals and Applications* (Eds.: M. Ghosh, K. L. Mittal), Marcel Dekker, **1996**, pp. 492 – 493.

